frontiers in Physics

ORIGINAL RESEARCH
published: 11 February 2022
doi: 10.3389/fphy.2022.806554

# Three-Dimensional Tunable Fibronectin-Collagen Platforms for Control of Cell Adhesion and Matrix Deposition

*Maryam Asadishekari[1†], Elie N. Mpoyi[1†], Yifan Li[2], Javad Eslami[1], Matthew Walker[3], Marco Cantini[3] and Delphine Gourdon[1,3]**

[1]Department of Physics, University of Ottawa, Ottawa, ON, Canada, [2]Department of Material Science and Engineering, Iowa State University, Ames, IA, United States, [3]Division of Biomedical Engineering, James Watt School of Engineering, University of Glasgow, Glasgow, United Kingdom

OPEN ACCESS

**Edited by:**
Oleg V. Kim,
University of Pennsylvania,
United States

**Reviewed by:**
Changjin Huang,
Nanyang Technological University,
Singapore
Donna Peters,
University of Wisconsin-Madison,
United States
Karin Wang,
Temple University, United States

***Correspondence:**
Delphine Gourdon
Delphine.Gourdon@glasgow.ac.uk

[†]These authors have contributed equally to this work

**Specialty section:**
This article was submitted to Biophysics, a section of the journal Frontiers in Physics

**Received:** 31 October 2021
**Accepted:** 14 January 2022
**Published:** 11 February 2022

**Citation:**
Asadishekari M, Mpoyi EN, Li Y, Eslami J, Walker M, Cantini M and Gourdon D (2022) Three-Dimensional Tunable Fibronectin-Collagen Platforms for Control of Cell Adhesion and Matrix Deposition. Front. Phys. 10:806554. doi: 10.3389/fphy.2022.806554

The extracellular matrix (ECM) is a complex fibrillar network that couples a cell with its environment and directly regulates cells' functions via structural, mechanical, and biochemical signals. The goal of this study was to engineer and characterize ECM-mimicking protein platforms with material properties covering both physiological and pathological (tumorous) tissues. We designed and fabricated three-dimensional (3D) fibrillar scaffolds comprising the two major components of the ECM, namely collagen (Col) and fibronectin (Fn), using a previously developed freeze-drying method. While scaffolds porous architecture and mechanics were controlled by varying Col I concentration, Fn deposition and conformation were tuned using varied immersion temperature and assessed *via* intramolecular Förster Resonance Energy Transfer (FRET). Our data indicate that all scaffolds were able to support various crucial cellular functions such as adhesion, proliferation and matrix deposition. Additionally, we show that, keeping the stiffness constant and tuning the conformation of the Fn layer used to coat the Col scaffolds, we were able to control not only the invasion of cells but also the conformation of the matrix they would deposit, from a compact to an unfolded structure (as observed in the breast tumor microenvironment). Therefore, these tunable scaffolds could be used as 3D cell culture models, in which ECM microarchitecture, mechanics and protein conformation are controlled over large volumes to investigate long-term mechanisms such as wound healing phases and/or vascularization mechanisms in both physiological and pathological (tumorous) microenvironments. These findings have implications for tissue engineering and regenerative medicine.

**Keywords: fibronectin (Fn), collagen type 1, three-dimensional scaffold, FRET, tumor-mimicking microenvironment**

## INTRODUCTION

Cells are known to sense and respond to the topography and mechanical properties of their substrates [1–3]. The difference in rigidity and microscale features of the extracellular matrix (ECM), such as protein conformation, is correlated with various cell behaviors including cell adhesion, migration, proliferation, as well as ECM deposition [4–6]. Fibronectin (Fn) is a key protein of the ECM with major roles in processes including wound healing and vascularization. Fn conformation could change upon cell traction, which in turn influences cell signaling consequently causing cancer

[7, 8]. Fn is critical to the deposition of collagen (Col) I based ECM [9] and its conformational changes serve as an indicator of increased tumor aggressiveness [10]. Förster resonance energy transfer (FRET) is a labeling method used as an indicator of Fn conformation (and Fn fiber strain) [11, 12]. External forces, applied *via* atomic force microscopes and laser tweezers, have been used to modify the conformation of individual protein molecules on two-dimensional (2D) substrates [13, 14]. Nevertheless, such force-induced protein stretching/unfolding methods have limitations as they can hardly apply in three-dimensional (3D) environments. Consequently, no investigation focusing on the control of Fn conformation in 3D templates based on natural protein, such as collagen, has been reported.

3D biomedical scaffolds have been shown to provide more physiologically relevant ECM-mimicking environments for cells than 2D substrates. 3D porous scaffolds are commonly used to replace or repair damaged tissues as they promote cell invasion and nutrients flow through interconnected pores [15–17]. While various materials are used to make 3D porous scaffolds, natural materials, such as proteins, are preferred due to their expected biocompatibility [18]. One of the most novel natural biomaterials currently used in cosmetic and drug delivery fields is Col, particularly type I. Col I is considered the gold standard in tissue engineering and regenerative medicine due to its biodegradability, biocompatibility and mechanical characteristics [19, 20]. It is mostly engineered in the fibrillar form or as sponges and sheets. One of the most popular collagen-based applications is wound dressings to cover the injuries and promote ulcer treatment [21–23]. Collagen-based biomaterials are categorized into two groups, decellularized ECMs, which mostly contain Col, or Col-based tissues. There are several common techniques to fabricate porous scaffolds including freeze-drying [24], which is an ideal technique to engineer protein-based scaffolds and was used in this study.

Research on how to better replicate and modify the microarchitecture of the ECM has long been the focus of intensive study due to its robust mechanical properties and moderate density, despite being comprised of relatively weak constituents. Tunable mechanics are often a limiting factor of Col scaffolds; these features are important in tissue engineering applications related to modeling changes in disease tissue, such as cancer, to elicit sufficient changes in cell traction forces for understanding pathologies associated with altered cell mechanosensing. Porous collagen scaffolds provide excellent substrates for protein adsorption, specifically Fn, and hence serve as an ECM-mimicking 3D platform to host cells for long-term in large volume media. The synergistic interplay between scaffold mechanics and presentation of Col-Fn can significantly regulate cell behavior to create functional divergence between pathologically relevant cell subsets. Indeed, in 2D, Avery et al. fabricated both compliant 2 kPa and stiff 20 kPa polyacrylamide gels modified with Col 1-Fn to assess myofibroblast differentiation using markers $\alpha$-smooth muscle actin ($\alpha$-SMA) and fibroblast activation protein (FAP). Compliant Fn-rich gels induced a contractile and proliferative phenotype expressing high FAP and low $\alpha$-SMA, whereas stiff and/or Col I-rich matrices induced overexpression of genes associated with ECM synthesis and proteolysis with low FAP and high $\alpha$-SMA expression [25]. Investigating the regulation of cell response in a 3D environment with controlled mechanics, microarchitecture and Col/Fn presentation would be highly informative physiological and pathological models, in addition of being innovative when Fn conformation can also be controlled.

In this work, we report the fabrication of 3D collagen scaffolds with controlled mechanics, microarchitecture and protein contents prepared *via* an ice-templating method; these are capable of supporting 3D cell cultures in large volumes and for long cell culture times. We first tuned the overall architecture and mechanics of our scaffolds by varying Col I concentration. Following Col I scaffold fabrication, we used varied temperature to control Fn conformation, which was assessed by intramolecular Förster Resonance Energy Transfer (FRET). The thermal method we applied to control the conformation of Fn molecules adsorbed onto the Col scaffolds did not affect the scaffolds bulk properties. This method allowed us to investigate cell invasion, viability and matrix deposition within Col-Fn scaffolds with tunable yet controlled properties. The resulting 3D scaffolds represent a versatile and powerful new platform to control Fn conformation (while keeping constant mechanics and microarchitecture) in tissue engineering and may pave new ways toward the development of useful tools for wound healing and mechanobiology research.

# MATERIALS AND METHODS

## Fabrication of 3D Collagen Type I Scaffolds

By use of the freeze-casting techniques, various Col scaffold with different porosity (microarchitecture) were produced. Scaffolds were fabricated from a suspension of type I Col microfibrillar derived from bovine tendon (Advanced BioMatrix) at concentrations from 0.5 wt% to 1.25 wt%. The suspension of type I Col was prepared in 0.05 M acetic acid solution (Sigma-Aldrich), and the pH was adjusted to 2.0 with hydrochloric acid (VWR International). The Col suspension was blended *via* an overhead homogenizer (T 10 BASIC S001) for 30 min in cold water bath and then, after mixing, centrifuged at 2,500 rpm for 15 min to remove air bubbles. The type I Col suspension was poured into rectangular Teflon molds, $10 \times 7 \times 2$ mm$^3$ in size. The samples were frozen in a freeze-dryer (VirTis Advantage Plus ES; SP Scientific; PA, United States) under constant temperature (−10°C) for 5 h, and then dried at the same temperature under 10 mTorr for 24 h.

## Chemical Crosslinking Treatment

To enhance the structural stability of the collagen scaffolds, the lyophilized samples were crosslinked with a water soluble carbodiimide. These scaffolds were immersed in a 95% ethanol solution containing 33 mM 1-ethyl-3-(3-dimethylamino propyl)-carbodiimide hydrochloride (EDC) (Sigma-Aldrich, United Kingdom) and 6 mM N-hydroxysuccinimide (NHS) (Sigma- Aldrich, United Kingdom) for 4 h at 25°C. Following the crosslinking process the scaffolds were washed thoroughly with distilled water (5 × 5 min) and were subsequently refrozen

and relyophilized using the controlled freezing temperature method detailed above.

## Structural Characterization of Collagen Scaffold Samples

The microstructure of Col scaffolds was quantified by scanning electron microscopy (SEM) and mercury intrusion porosimetry. SEM (Mira3 FESEM, Tescan) imaging of both bare Col scaffolds and cell-laden Col-Fn scaffolds was performed on Au/Pd sputtered samples at 15 keV. The pore size and distribution of the monolith sample were assessed by Hg intrusion porosimetry (Autopore IV 9500; Micromeritics). Monoliths were placed in glass penetrometers of known weight and volume, which were then mounted into the instrument. Analysis was performed using an automated procedure in which penetrometers were first evacuated to 50 μm Hg and then filled with Hg at 0.2 psi. Pressure applied to the column of Hg was ramped stepwise to 48 psi to probe pores with size greater than 4 μm in diameter. Seven samples were analyzed to calculate the median pore diameter and median pore volume in each condition. Monoliths were also characterized with a dynamic mechanical analyzer (DMA Q800; TA Instruments) to quantify the impact of Col concentration on scaffold mechanical properties. Col scaffolds were placed under compressive loads before and after being soaked in cell culture medium (*α*MEM, Sigma-Aldrich) overnight at room temperature. Measurements comprised a single loading cycle, with an initial contact force of 0.05 N and a ramp rate of 0.005 N/min up to 0.075 N. Compressive elastic modulus for the monoliths was calculated as the slope of the stress-strain curve over the 1–2% strain regime. Three samples per condition were analyzed to calculate the mean and standard deviation of the compressive moduli.

## Cell Culture Experiments

Scaffolds were cut into 1 mm thick slices and prepared for cell culture experiments. They were first placed under UV light during 30 min for disinfection and rinsed 3 times with sterile PBS (Life Technologies). The scaffolds were then immersed in a solution of Fn at 50 μg/ml and placed for an hour either at 4 or 37°C before seeding with 3T3-L1 cells (ATCC #CL-173) or GFP-labeled 3T3 cells, an adipogenic subtype of mouse fibroblasts. The cells were incubated in *α*MEM (Sigma-Aldrich) containing 10 vol % fetal bovine serum (FBS, Tissue Culture Biologicals) and 1 vol% penicillin/streptomycin (pen/strep) (Life Technologies) prior to seeding. The cells were seeded in 10 μL suspensions (containing 30,000 cells) on the top of the prepared scaffolds and were allowed to adhere for 1 h. Then, fresh media containing 1 vol% fetal bovine serum (FBS, Tissue Culture Biologicals) was added to the scaffolds that were finally placed in an incubator at 37°C (5% $CO_2$) for either 12 or 24 h.

## Cell Invasion and Viability

The cell-loaded scaffolds were rinsed twice in PBS after culture and soaked in 3.7% ice-cold paraformaldehyde for chemical fixation. To assess cell invasion and adhesion in the scaffolds, the samples were stained with 4′,6-diamidino-2-phenylindole (DAPI), calcein AM, and propidium iodide (PI) (all from Life Technologies), and later imaged *via* laser scanning fluorescence confocal microscopy (Zeiss710, Zeiss, Munich, Germany) using a 10X/0.25 objective. The number of cells was quantified *via* ImageJ on six random spots of three different samples per condition.

The viability of the 3T3-L1s was assessed with a Live/Dead Viability/Cytotoxicity Kit (Molecular Probes, OR) after 24 h, 48 h and/or 7 days of culture. The unfixed samples were rinsed twice in PBS and incubated in Live/Dead working solution, containing 2 μM calcein AM and 4 μM EthD-1, for 30 min in the incubator at 37°C, 5% CO2. Images were acquired by laser scanning fluorescence confocal microscopy (Zeiss710, Zeiss, Munich, Germany) using a 10X/0.25 objective, and the number of cells was quantified *via* ImageJ on six random spots of three different samples per condition.

## Fibronectin and FRET Labeling

Fn was acquired from Life Technologies, NY. For intramolecular FRET experiments, Alexa Fluor 488 succinimidyl ester and Alexa Fluor 546 maleimide fluorophores (Invitrogen, CA) were used to dual-label Fn, as described in previous work [11]. Labeling ratios and Fn concentrations were obtained using a DU®730 UV/Vis spectrophotometer (Beckman, IN) at 280, 495, and 556 nm. Calibration of FRET-labeled Fn was performed in guanidine hydrochloride (GdnHCl) solution at concentrations of 0, 2, and 4 M to calculate FRET ratios, defined as acceptor/donor intensity ratios, and as a function of protein denaturation.

To assess FRET on scaffolds, Col scaffolds were thoroughly rinsed with PBS and then coated with a 50 μg/ml Fn solution containing 10% FRET-labeled Fn, for 24 h. After incubation, the samples were gently washed with PBS and kept in PBS before cell seeding. For visualization of new Fn matrix deposited by cells, the Col scaffolds were first coated with a 50 μg/ml unlabeled Fn solution for 24 h then the samples were rinsed with PBS and a new solution containing 10% FRET-labeled Fn was added with the fresh cell culture media right after cell seeding and placed in the incubator for 48 h.

## FRET Data Analysis

Fn-adsorbed scaffolds were imaged with a Zeiss 710 laser scanning fluorescence confocal microscope (Zeiss, Munich, Germany). Z-stack images were obtained in 16-bit using the C-Apochromat water-immersion 40×/1.2 objective, with the pinhole of one AU, pixel dwell time of 6.3 μs, photomultipliers (PMTs) gains set at 500 V, and z-step size of 1 μm. FRET-labeled Fn was excited with a 488 nm laser line; emissions from donor ($I_{DON}$) and acceptor ($I_{ACC}$) fluorophores were simultaneously collected in the PMT1 channel (514–526 nm) and the PMT2 channel (566–578 nm), respectively. These z-stack images were analyzed with user-defined Matlab code to generate both the mean FRET ratios ($I_{ACC}/I_{DON}$) and the Fn amounts adsorbed ($I_{ACC} + I_{DON}$) at each location [5, 11]. Six different random spots per sample and three samples per condition were analyzed to calculate the mean and standard deviation of the FRET intensities.

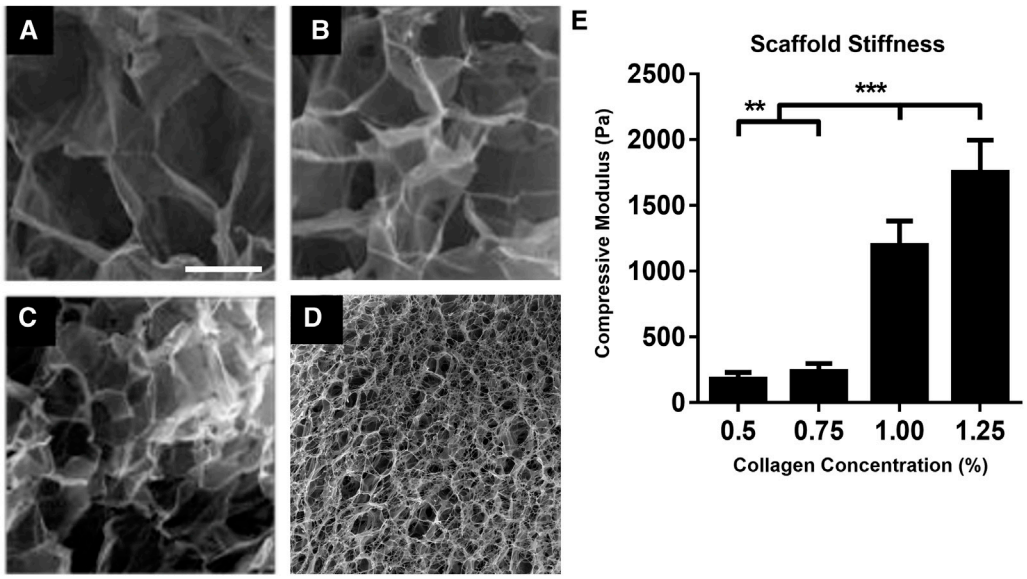


**FIGURE 1 |** Collagen concentration governs microarchitecture and mechanics of scaffolds. SEM micrographs of porous Col scaffolds fabricated *via* ice-templating at −10°C using 0.5 wt% **(A)**, 0.75 wt% **(B)**, 1.0 wt% **(C)** and 1.25 wt% **(D)** Col concentrations. Compressive modulus of corresponding Col scaffolds, as measured *via* DMA **(E)**. $^{**}p < .01$, $^{***}p < .001$, Mean ± SD. Scale bar = 100 μm.

## Confocal Reflectance Microscopy Imaging

To visualize the microarchitecture of the underlying collagen scaffolds concomitantly to FRET imaging, confocal reflectance imaging was performed following FRET imaging by illuminating the same field of view with a low intensity 488 nm laser line and the backscatter light reflected from the collagen was collected in a third photomultiplier tube (PMT3). Z-stack images were analysed *via* ImageJ.

## Statistical Analysis

One-way ANOVA with Tukey's posttest, Dunnett's posttest and Student's t-test were used to determine statistical significance between conditions in GraphPad Prism (GraphPad Software, California United States). In all cases, $p < .05$ is indicated by a single star (*), $p < .01$ by a double star (**), and $p < .001$ by three stars (***).

# RESULTS

## Effect of Collagen Concentration on Scaffolds Microarchitecture and Mechanics

To investigate the effect of Col concentration on scaffold pore size, pore distribution and mechanical properties, all scaffolds fabricated *via* ice-templating at −10°C with varied Col concentrations (0.5, 0.75, 1.0 and 1.25 wt%) were analyzed using SEM, Hg intrusion porosimetry and DMA, respectively. SEM images indicate the presence of an interconnected porous network in all scaffolds, with pore size decreasing as Col concentration increased, as well as more uniform pores visible at the highest (1.25 wt%) Col concentration (**Figures 1A–D**). Next, we quantified scaffolds compressive moduli by acquiring stress-strain profiles *via* DMA. Our data show that moduli significantly increased with increasing Col concentration, from 200 ± 30 Pa at 0.5 wt% to 1700 ± 300 Pa at 1.25 wt% (**Figure 1E**). As expected, larger pore sizes correlated with lower compressive moduli, as the 3D structural integrity of the scaffolds was compromised when pores collapsed. Additionally, Hg porosimetry (**Supplementary Figure S1**) allowed us to quantify pore size more accurately and confirmed that it decreased from circa 214–35 μm in diameter when Col concentration increased from 0.5 wt% to 1.25 wt% (**Table 1**). Hg porosimetry also proved that pores are indeed interconnected to allow for Hg intrusion within the whole 3D structure.

**TABLE 1 |** Microporosity of collagen scaffolds as quantified by Hg intrusion porosimetry.

| Collagen concentration (wt%) | Median pore diameter (μm) | Median pore volume (ml/g) |
|---|---|---|
| 0.5 | 214.4 ± 12.2 | 36.2 ± 1.8 |
| 0.75 | 147.1 ± 8.1 | 31.8 ± 1.2 |
| 1.0 | 74.0 ± 3.0 | 22.0 ± 0.9 |
| 1.25 | 35.9 ± 2.7 | 18.9 ± 0.8 |

After extensive characterization of the four types of scaffolds in presence of cells, because the 1.25 wt% Col series exhibited not only better cell invasion and overall cell distribution (**Supplementary Figure S2**) but also lower swelling and higher stability over time (data not shown) than the other three Col series, they were chosen for all further cell experiments. The enhanced attachment and invasion of cells within the 1.25 wt% Col scaffolds is likely due to their higher compressive modulus promoting higher cell-generated forces and to greater presentation of integrin binding sites within the increased collagen amounts.

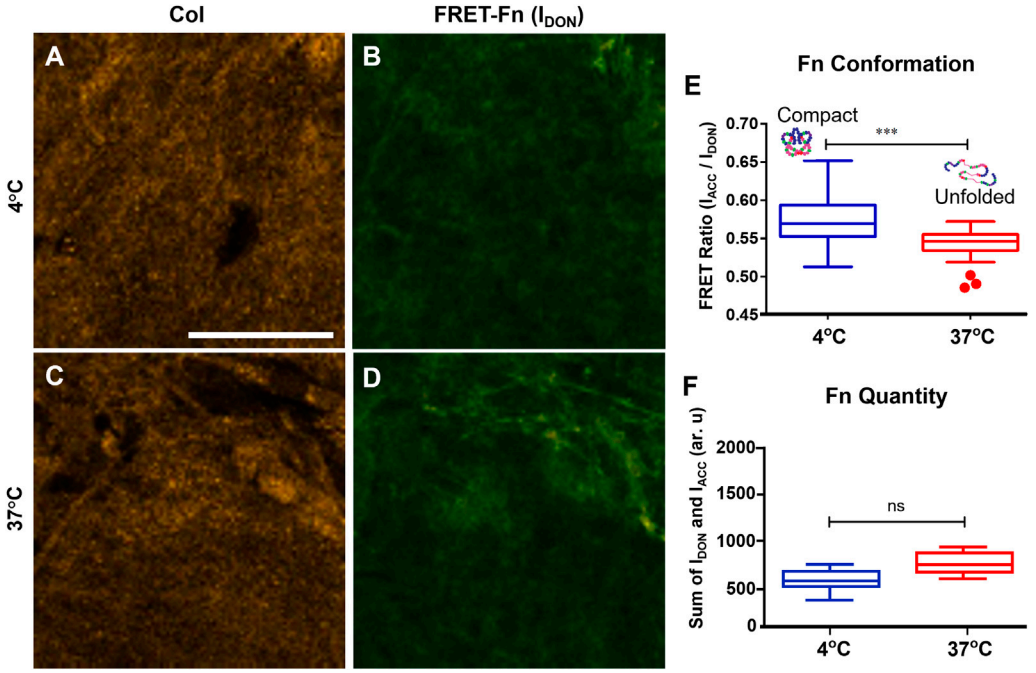


**FIGURE 2 |** Temperature controls the conformation of fibronectin coating onto collagen scaffolds. Confocal reflectance microscopy (CRM) image of Col **(A)** and fluorescence image (donor channel) of FRET-labeled Fn coating **(B)** of the same field of view of a scaffold coated at 4°C. Same imaging method/channels for a scaffold coated at 37°C **(C,D)**. Mean FRET ratios ($I_{ACC}/I_{DON}$) highlighting the significant difference between Fn adsorbed onto the 4°C scaffold (0.57 ± 0.03) characteristics of compact Fn conformations and Fn adsorbed onto the 37°C scaffold (0.53 ± 0.02) characteristics of unfolded Fn conformations **(E)**. Total quantity of Fn adsorbed ($I_{ACC}$ + $I_{DON}$) onto both scaffolds indicating no difference in Fn amount/density between 4 and 37°C conditions **(F)**. ***$p$ < .001, Student's t-test, Mean ± SD. Scale bar = 30 μm.

## Control of Fibronectin Coating Conformation

To control Fn conformation on the Fn-Col porous scaffolds (1.25 wt % Col), two different immersion temperatures were used. The effect of temperature on Fn conformation was quantified by soaking the Col scaffolds in Fn solutions containing trace amounts of FRET labeled Fn (to avoid intermolecular FRET) for an hour either at 4°C or at 37°C, after which all scaffolds were placed in an incubator for 24 h. Underlying Col and FRET-Fn coating were then imaged sequentially *via* confocal reflectance and confocal fluorescence microscopy (CRM), respectively (**Figures 2A–D**). Fn conformations and quantities were assessed *via* intramolecular FRET imaging [11, 26, 27]. Fn coating on scaffolds placed at 4°C indicated high mean FRET ratios suggesting Fn molecules were in a close-to-compact conformation, while Fn coating on scaffolds at 37°C showed significantly lower mean FRET ratios suggesting the presence of partially unfolded Fn conformations (**Figure 2E**). These findings are consistent with results obtained on 2D surfaces (data previously observed in our lab, not shown), which further demonstrates our ability to tune Fn conformation on demand using varied immersion temperatures in both 2D and 3D environments. Additionally, no significant difference in total Fn fluorescence intensity was detected between conditions, which indicates that the average amount of adsorbed Fn per unit area (density) was similar on both 4 and 37°C scaffolds (**Figure 2F**).

## Effect of Fibronectin Coating Conformation on Cell Invasion and Short-Term Viability

To investigate whether differences in Fn conformation within the Fn-Col scaffolds affected cell invasion and subsequent viability, 30 k GFP-3T3 cells were seeded on top of scaffolds that were initially immersed in Fn solution and placed either at 4 or at 37°C, as described above, with an additional control sample simply immersed in PBS at room temperature (no Fn coating). All scaffolds were then incubated for 24 h. Our confocal imaging data indicate that the GFP-labeled mouse fibroblast 3T3 cells successfully invaded (up to 500 μm deep) the scaffolds showing also a relatively homogeneous cell distribution from top to bottom of the samples (**Figures 3A–C**). This indicated that cells were able to adhere and migrate through these high Col concentration porous scaffolds having very small pore size.

As Fn conformation plays a key role in guiding numerous cell functions, we next performed a viability assay after 24 h incubation using 3T3-L1 fibroblast cells because of their active role in migration and matrix assembly *in vitro* [28]. Live/Dead staining of cells indicated very few dead cells (**Figures 3D–F**): our data show a clear trend with higher viability, above 93%, in scaffolds coated with Fn than in bare Col scaffolds [and a slight preference for compact Fn coating (4°C) with respect to unfolded Fn coating (37°C)], although no significant difference was measured (**Figure 3G**). Importantly, we did not notice any

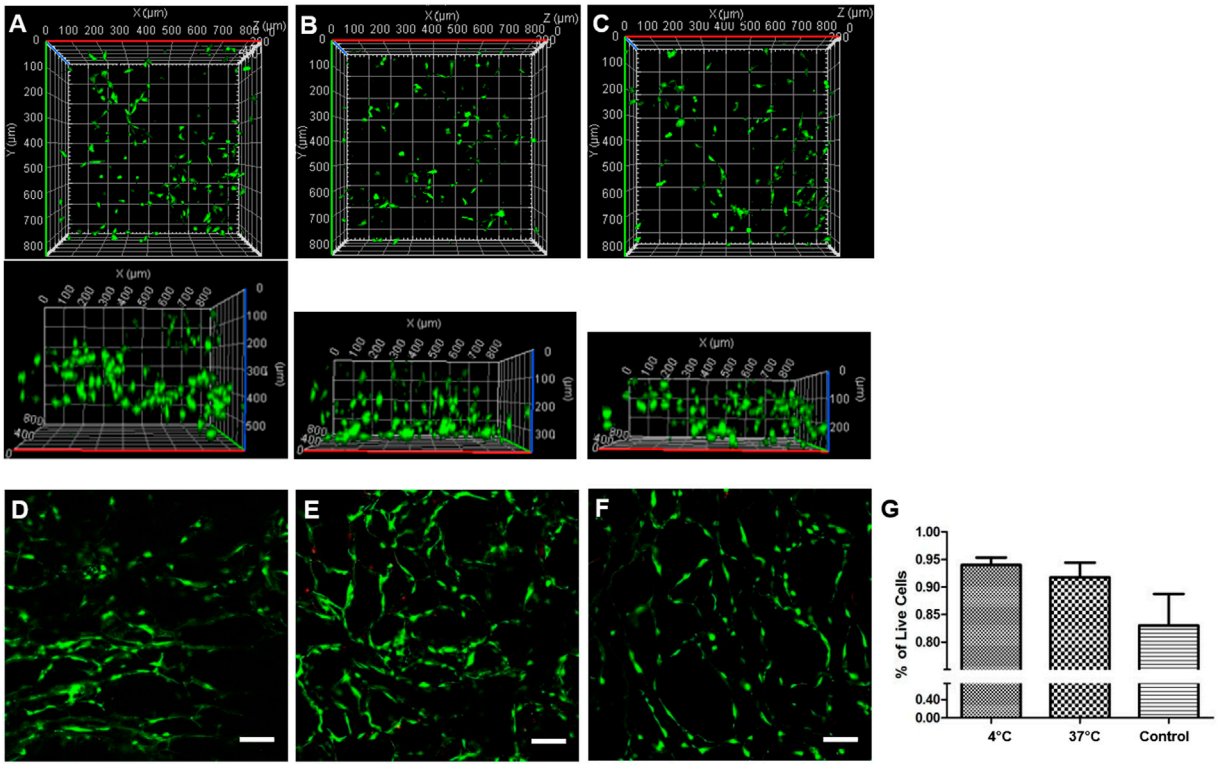


**FIGURE 3 |** Fibronectin coating conformation affects cell invasion and viability. 3D view of GFP-labeled 3T3 cells distribution within Col scaffolds initially coated with Fn at 4°C **(A)**, 37°C **(B)**, or left in PBS (control, no Fn) at room temperature **(C)** prior to seeding. 3T3-L1 cells viability was quantified *via* Live/Dead assay for all scaffolds, at 4°C **(D)**, at 37°C **(E)** or control **(F)** after 24 h incubation. Live cells were stained with calcein (green), and dead cells were stained with propidium iodide (red). Scale bar = 100 μm. Live cells number per volume was quantified in percentage for all scaffolds **(G)**.

significant difference in viability between top and bottom of scaffolds. Collectively, these results indicate that these Col-Fn porous scaffolds provide an excellent environment for cells to interact with, invade, and remain viable, proving scaffolds' biocompatibility.

## Long-Term Cell Viability and Matrix Assembly Within Col-Fn Scaffolds

To assess whether our Fn-Col scaffolds could potentially be used as platforms for long-term cell cultures, we next assessed long-term cell viability and subsequent cells' ability to assemble and deposit their own ECM. 3T3-L1 cells (30 k cells/scaffold) were seeded on top of 4°C Fn-Col scaffolds in DMEM media containing 1% FBS. After an hour, the media was replaced with DMEM containing 10% FBS with an addition of 0.05 mg/ml exogeneous unlabeled Fn for cells to incorporate and facilitate fibrillogenesis. Scaffolds were then incubated either for 48 h or 7 days (in which case Fn-supplemented medium was exchanged every other day). Further, a fluorescent viability assay of unfixed scaffolds indicated that most cells were viable not only after short-term (48 h, **Figure 4A**) but also long-term (7 days, **Figure 4B**) culture. To assess whether the 3T3-L1s were properly distributed within the monoliths, the interior of chemically fixed (crosslinked) scaffolds were revealed by cryo-ultramicrotome sectioning, and subsequent SEM imaging showed that cells successfully invaded the scaffold and adhered to the Fn-coated Col architectures (**Figure 4C**). Finally, further SEM imaging of a similar scaffold after decellularization showed clearly visible protein fibers across the porous structure, indicating that 3T3-L1s were performing regular cell functions such as the assembly of an ECM (**Figure 4D**).

## Effect of Fibronectin Coating on the Conformation of Cell-Deposited Matrix Fibers

To investigate further whether matrix assembly (including matrix conformation) could be controlled, Col scaffolds were first coated with a 50 μg/ml unlabeled Fn solution for 1 h either at 4 or at 37°C, then placed for 24 h in the incubator. The samples were then rinsed with PBS. 3T3-L1 cells (30 k cells/scaffold) were seeded on top of both scaffolds in DMEM media containing 1% FBS. After an hour, the media was replaced with DMEM containing 10% FBS with an addition of 50 μg/ml Fn including 10% FRET-labeled Fn for cells to incorporate and samples were incubated for 48 h. Underlying Col and FRET-Fn fibers were then imaged sequentially *via* confocal reflectance and confocal fluorescence microscopy (CRM), respectively (**Figures 5A–D**). The mean FRET ratio measured on fibers deposited onto 4°C

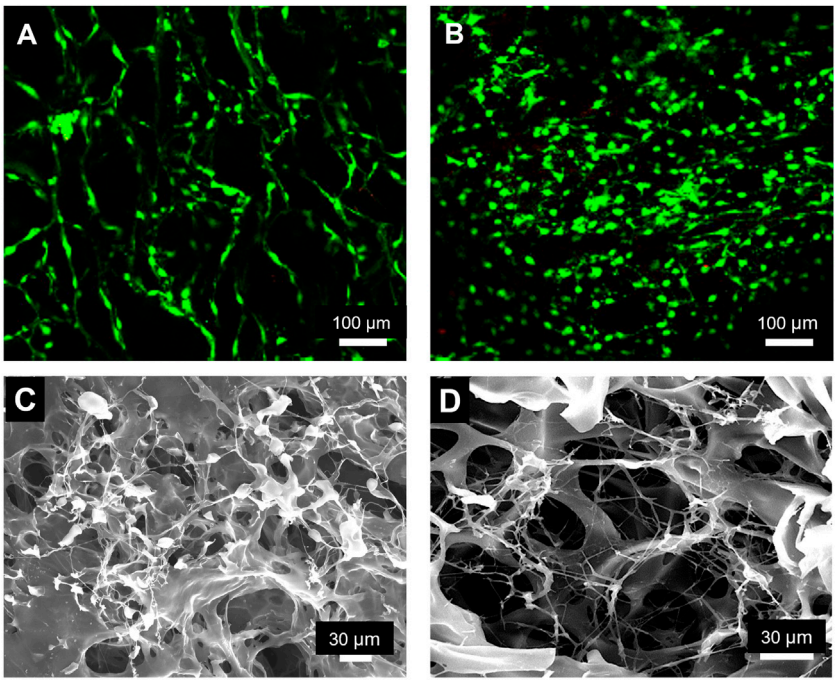


**FIGURE 4 |** Fibronectin coated collagen scaffolds support long-term cell viability and matrix deposition by 3T3-L1 cells. Fluorescence micrograph of a Col scaffold coated with Fn at 4°C after 48 h **(A)** and 7 days **(B)** of 3T3-L1 culture, showing very high cell viability. Live cells were stained with calcein (green) and dead cells with propidium iodide (red). SEM micrograph of a similar scaffold after 48 h of cell culture, indicating invasion of the scaffold by 3T3-L1s **(C)**. SEM image of a decellurarized scaffold, clearly showing an extended network of protein fibers produced by 3T3-L1 cells during 48 h of culture **(D)**.

scaffolds was significantly higher than that measured on fibers deposited onto 37°C scaffolds (**Figure 5E**). These results suggest that, in our Col-Fn scaffolds, the underlying compact Fn coating (4°C condition) promotes the deposition of rather compact/relaxed Fn fibers, while the underlying unfolded Fn coating (37°C condition) favors the assembly of more unfolded and stretched Fn fibers. Additionally, no significant difference in total Fn fluorescence intensity was detected between conditions, which indicates that the average amount of fibrillar Fn per unit area (density) was similar on both 4 and 37°C scaffolds (**Figure 5F**). These findings are consistent with previous studies [12] and are discussed in next section.

Collectively, our results indicate 1) that we were able to engineer 3D ECM-mimicking platforms in which only one parameter (here Fn conformation) can be tuned while all others parameters (scaffold rigidity, microarchitecture, pore size/connectivity, etc.) are kept constant, 2) that cells can sense the underlying Fn conformation of the scaffold coating and 3) that cells can respond to these conformational variations by depositing matrix fibers exhibiting varied molecular conformation (at least during the first 48 h in culture).

## DISCUSSION

In this study, we fabricated 3D Col porous scaffolds by freeze-casting, a relatively cheap and easy way of producing scaffolds with controlled pore size for different types of materials such as ceramics [25], polymers [29], collagen [28] and gelatin [30]. As expected, pore size was found to decrease with increased Col concentration. Increased collagen content occupies more space within the Teflon mold, which leads to smaller ice crystals, explaining the decrease in pore size (which mirrors ice crystal structure) with increased collagen concentration. Among all samples, the compressive modulus of the 1.25 wt% Col porous scaffolds used in our study was 1720 ± 300 Pa, indicating a suitable stiffness match with a variety of tissues *in vivo* [31]. Although the scaffolds were chemically cross-linked to retain cohesiveness and long-term stability in aqueous environments, their biocompatibility was demonstrated, as large populations of cells could successfully invade and proliferate within the structures, remaining viable over long-term cultures (7 days), in part due to the presence of large interconnected pores that facilitated their migration and communication. Additionally, the relatively high rigidity of 1.25 wt% Col scaffolds promoted better cell invasion and distribution, likely due to enhanced cell-generated forces and greater presentation of integrin binding sites within the increased collagen amounts per unit volume.

A major accomplishment of this work was to generate scaffolds with controlled microarchitecture and rigidity but also with tunable protein conformation, this was achieved by coating the Col porous scaffolds with a layer of Fn using a 1 h immersion at either cold (4°C) or warm (37°C) temperatures to tune Fn conformation. With this method, we successfully obtained two categories of Col-Fn scaffolds with controlled protein conformation: compact Fn coated scaffolds (as

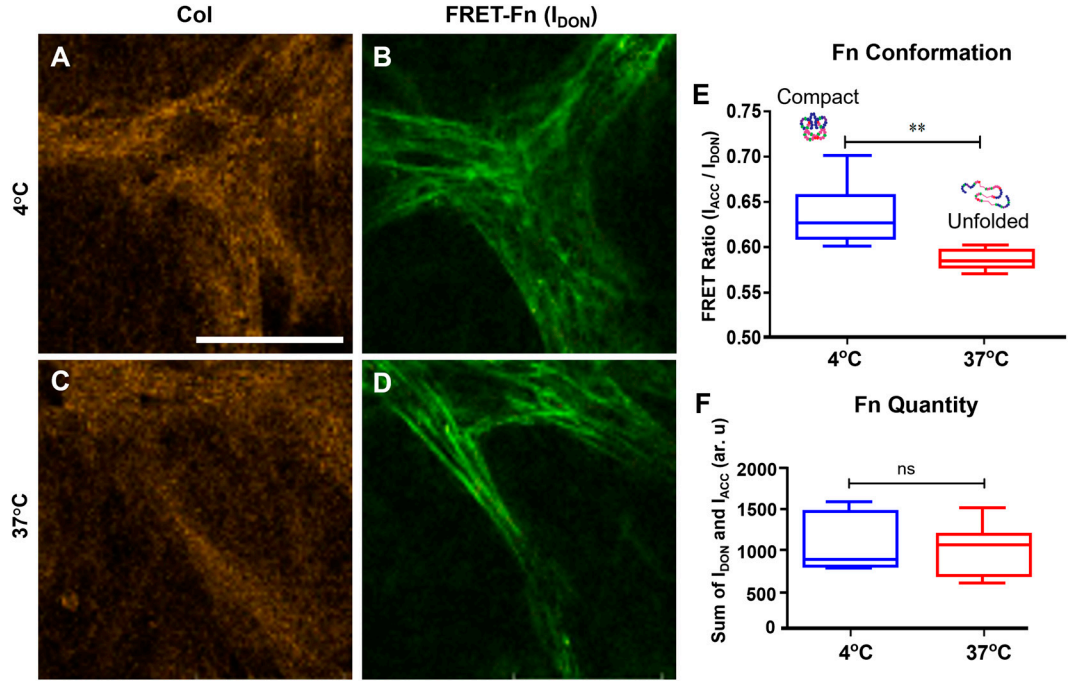


**FIGURE 5 |** Fibronectin coating dictates the conformation of the new matrix deposited by 3T3-L1s after 48 h incubation. Confocal reflectance microscopy (CRM) image of Col **(A)** and fluorescence image (donor channel) of FRET-labeled cell-deposited Fn fibers **(B)** of same field of view of a scaffold coated at 4°C. Same imaging method/channels for a scaffold coated at 37°C **(C,D)**. Mean FRET ratios ($I_{ACC}/I_{DON}$) highlighting the significant difference between Fn fibers formed on the 4°C scaffold (0.64 ± 0.03) comprising more compact Fn conformations than Fn fibers on the 37°C scaffold (0.59 ± 0.02) in which unfolded Fn conformations are also present **(E)**. Total quantity of Fn ($I_{ACC}$ + $I_{DON}$) detected onto both scaffolds indicating similar Fn amount/density between 4 and 37°C conditions **(F)**. ***$p$ < .001, Student's t-test, Mean ± SD. Scale bar = 30 μm.

assessed by high FRET ratios, obtained at 4°C deposition) and unfolded Fn coated scaffolds (as assessed by low FRET ratios, obtained at 37°C deposition). Interestingly, both 4 and 37°C coated scaffolds could partially retain compact and unfolded conformations, respectively, even after 24 h incubation (time point at which cells were seeded for viability and matrix deposition studies). We attribute the "partial" retention of Fn conformation to 1) the specific interactions of Fn with the underlying Col surface and 2) the intermolecular forces within the Fn layer. We previously calibrated such effect on flat mica substrates (data not shown) by comparing FRET right after 1 h immersion of Fn either at 4 or 37°C and after 24 h incubation. Our data indicated that 1) FRET decreased in both 4 or 37°C coatings after 24 h of incubation, which was expected due to temperature/entropy induced unfolding but also that 2) the FRET difference between 4 and 37°C samples was maintained, with 4°C coatings systematically retaining a more compact (higher FRET) conformation than 37°C coatings, as observed in the present study. Our observations are also consistent with previous results obtained on hydroxyapatite crystals and 2D Fn-coated coverglass chambers, where Fn conformation versus temperature followed the same trend [5, 32].

Col scaffolds coated with Fn showed increased cell invasion and survival, with a preference for low-temperature prepared scaffolds (coated with compact Fn) [1, 33]. These data suggest that cells favor interactions with compact Fn scaffolds likely because they can use their most common integrins type, $\alpha_5\beta_1$, while they have to rely on less common (and less numerous) $\alpha_V\beta_3$ integrins to bind to unfolded Fn scaffolds, due to their inability to engage simultaneously the RGD sequence and the synergy site, located on the $FnIII_{10}$ and $FnIII_9$ modules of Fn, respectively when Fn is extended or unfolded [34–37].

Finally, the ability of cells to perform not only regular cell functions such as adhesion and proliferation but also matrix assembly with fibers exhibiting controlled conformation (compact/relaxed Fn fibers were deposited within compact Fn coated Col scaffolds while unfolded/stretched Fn fibers were deposited within unfolded Fn coated Col scaffolds) demonstrates the high level of control over ECM properties we could reach at early stages of cell culture (48 h). The dependence of the physical and biochemical characteristics of newly deposited Fn on the conformation (and rigidity) of a pre-existing underlying Fn network was first demonstrated in a study by Kubow and coworkers [38]. The authors proposed that the stretching/unfolding of fibers would upregulate the binding of soluble Fn, which could at least in part be due to the exposure of cryptic sites on FnIII modules involved in regulating Fn fibrillogenesis (in particular the matricryptic site within $FnIII_1$). Additionally, as unfolded Fn fibers also exhibit higher rigidity, this tended to increase the contractility of interacting cells (molecular clutch model), consequently leading to the deposition of a stiffer (hence more stretched/unfolded) matrix.

Collectively, our findings suggest that the Fn coated Col scaffolds we generated provide a satisfying 3D environment for fibroblasts to attach, grow, and function normally, over long-term cell cultures, which fulfilled the essential criteria for an *in vivo* mimicking 3D cell-culture platform based on collagen. Therefore, these tunable Col-Fn scaffolds could be used as 3D cell culture models, in which ECM microarchitecture, mechanics and protein conformation are controlled over large volumes to investigate long-term mechanisms such as wound healing phases and/or vascularization mechanisms in both physiological (compact Fn category) and tumorous [32] (unfolded Fn category) microenvironments.

## CONCLUSION AND FUTURE WORK

In this study, we have designed and engineered 3D porous Fn-coated Col scaffolds in which Fn conformation could be thermally switched from close-to-compact to (partially) unfolded. Those tunable Fn-Col scaffolds proved to regulate various key cell functions. Our results indicate that underlying Fn conformation could direct cell adhesion and early matrix deposition, as cells interacting with Fn in compact conformation generated a more compact/relaxed matrix than cells in contact with unfolded Fn, which deposited a more stretched and unfolded matrix. Such scaffolds potentially provide ECM-mimicking substrates for cells that can dictate and monitor cell functions. The use of those porous scaffolds in the context of wound healing or skin graft requires further investigations of cell behavior including migration assay and quantification of key growth factors such as TGF, FGF and VGEF. In conclusion, in this study, we have fabricated 3D Fn-Col platforms which composition, microarchitecture and mechanics quite accurately recapitulate the cell-deposited ECM. The additional level of control we achieved over Fn molecular conformation makes these platforms of potential use in cancer research, as they can easily be switched from a compact/relaxed state to an unfolded state, as reported in physiological and tumorous conditions, respectively. Therefore, these tunable Fn-Col scaffolds provide promising physiologically and pathologically relevant 3D platforms to monitor cell functions for long-term and large volume cells assays, with implications for tissue engineering and regenerative medicine.

## DATA AVAILABILITY STATEMENT

The raw data supporting the conclusion of this article will be made available by the authors, without undue reservation.

## AUTHOR CONTRIBUTIONS

MA and EM contributed equally to this work YL and DG conceptualized the idea and designed the project. YL performed fabrication and mechanical characterization of the collagen scaffolds. MA and EM performed FRET experiments and analyzed fibronectin conformation, whereas MA, EM, and JE performed and analyzed *in vitro* cellular studies. MA, EM, JE, MW, MC, and DG wrote the manuscript. All authors contributed to revising the manuscript. DG supervised the project.

## FUNDING

This research was supported by the Natural Sciences and Engineering Research Council of Canada (NSERC) under the Discovery Grant award RGPIN−2017−06784 and the Royal Society of the United Kingdom under the Wolfson award RSWF/FT/191020.

## SUPPLEMENTARY MATERIAL

The Supplementary Material for this article can be found online at: https://www.frontiersin.org/articles/10.3389/fphy.2022.806554/full#supplementary-material

## REFERENCES

1. Ngandu Mpoyi E, Cantini M, Reynolds PM, Gadegaard N, Dalby MJ, Salmerón-Sánchez M. Protein Adsorption as a Key Mediator in the Nanotopographical Control of Cell Behavior. *ACS Nano* (2016) 10: 6638–47. doi:10.1021/acsnano.6b01649
2. Vogel V, Sheetz M. Local Force and Geometry Sensing Regulate Cell Functions. *Nat Rev Mol Cel Biol* (2006) 7:265–75. doi:10.1038/nrm1890
3. Ron A. Mechano-Molecular Transduction: Putting the Pieces Together. *Biophys Chem* (2018) 241:15–9. doi:10.1016/j.bpc.2018.07.007
4. Dalby MJ. Topographically Induced Direct Cell Mechanotransduction. *Med Eng Phys* (2005) 27:730–42. doi:10.1016/j.medengphy.2005.04.005
5. Wu F, Chen W, Gillis B, Fischbach C, Estroff LA, Gourdon D. Protein-crystal Interface Mediates Cell Adhesion and Proangiogenic Secretion. *Biomaterials* (2017) 116:174–85. doi:10.1016/j.biomaterials.2016.11.043
6. Yeung T, Georges PC, Flanagan LA, Marg B, Ortiz M, Funaki M, et al. Effects of Substrate Stiffness on Cell Morphology, Cytoskeletal Structure, and Adhesion. *Cell Motil. Cytoskeleton* (2005) 60:24–34. doi:10.1002/cm.20041
7. Wang JH-C, Lin J-S. Cell Traction Force and Measurement Methods. *Biomech Model Mechanobiol* (2007) 6:361–71. doi:10.1007/s10237-006-0068-4
8. Yang L, Witten TM, Pidaparti RM. A Biomechanical Model of Wound Contraction and Scar Formation. *J Theor Biol* (2013) 332:228–48. doi:10.1016/j.jtbi.2013.03.013
9. Anderson JM. Biological Responses to Materials. *Annu Rev Mater Res* (2001) 31:81–110. doi:10.1146/annurev.matsci.31.1.81
10. Sethi T, Rintoul RC, Moore SM, MacKinnon AC, Salter D, Choo C, et al. Extracellular Matrix Proteins Protect Small Cell Lung Cancer Cells against Apoptosis: A Mechanism for Small Cell Lung Cancer Growth and Drug Resistance *In Vivo*. *Nat Med* (1999) 5:662–8. doi:10.1038/9511
11. Wang K, Wu F, Seo BR, Fischbach C, Chen W, Hsu L, et al. Breast Cancer Cells Alter the Dynamics of Stromal Fibronectin-Collagen Interactions. *Matrix Biol* (2017) 60-61:86–95. doi:10.1016/j.matbio.2016.08.001

12. Kubow KE, Vukmirovic R, Zhe L, Klotzsch E, Smith ML, Gourdon D, et al. Mechanical Forces Regulate the Interactions of Fibronectin and Collagen I in Extracellular Matrix. *Nat Commun* (2015) 6:1–11. doi:10.1038/ncomms9026
13. Fisher TE, Oberhauser AF, Carrion-Vazquez M, Marszalek PE, Fernandez JM. The Study of Protein Mechanics with the Atomic Force Microscope. *Trends Biochem Sci* (1999) 24:379–84. doi:10.1016/s0968-0004(99)01453-x
14. Mehta AD, Rief M, Spudich JA, Smith DA, Simmons RM. Single-Molecule Biomechanics with Optical Methods. *Science* (1999) 283:1689–95. doi:10.1126/science.283.5408.1689
15. Zhang X, Li C, Luo Y. Aligned/Unaligned Conducting Polymer Cryogels with Three-Dimensional Macroporous Architectures from Ice-Segregation-Induced Self-Assembly of PEDOT-PSS. *Langmuir* (2011) 27:1915–23. doi:10.1021/la1044333
16. Davidenko N, Gibb T, Schuster C, Best SM, Campbell JJ, Watson CJ, et al. Biomimetic Collagen Scaffolds with Anisotropic Pore Architecture. *Acta Biomater* (2012) 8:667–76. doi:10.1016/j.actbio.2011.09.033
17. Shahini A, Yazdimamaghani M, Walker KJ, Eastman MA, Hatami-Marbini H, Smith BJ, et al. 3D Conductive Nanocomposite Scaffold for Bone Tissue Engineering. *Int J Nanomed.* (2014) 9:167–81. doi:10.2147/IJN.S54668
18. Shin H, Jo S, Mikos AG. Biomimetic Materials for Tissue Engineering. *Biomaterials* (2003) 24:4353–64. doi:10.1016/s0142-9612(03)00339-9
19. Yannas IV, Burke JF, Orgill DP, Skrabut EM. Wound Tissue Can Utilize a Polymeric Template to Synthesize a Functional Extension of Skin. *Science* (1982) 215:174–6. doi:10.1126/science.7031899
20. Lauer-Fields JL, Kele P, Sui G, Nagase H, Leblanc RM, Fields GB. Analysis of Matrix Metalloproteinase Triple-Helical Peptidase Activity with Substrates Incorporating Fluorogenic L- or D-Amino Acids. *Anal Biochem* (2003) 321:105–15. doi:10.1016/s0003-2697(03)00460-3
21. Chocarro-Wrona C, López-Ruiz E, Perán M, Gálvez-Martín P, Marchal JA. Therapeutic Strategies for Skin Regeneration Based on Biomedical Substitutes. *J Eur Acad Dermatol Venereol* (2019) 33:484–96. doi:10.1111/jdv.15391
22. Dai C, Shih S, Khachemoune A. Skin Substitutes for Acute and Chronic Wound Healing: an Updated Review. *J Dermatol Treat* (2020) 31:639–48. doi:10.1080/09546634.2018.1530443
23. Liu Y, Panayi AC, Bayer LR, Orgill DP. Current Available Cellular and Tissue-Based Products for Treatment of Skin Defects. *Adv Skin Wound Care* (2019) 32:19–25. doi:10.1097/01.asw.0000547412.54135.b7
24. Lungu A, Albu MG, Stancu IC, Florea NM, Vasile E, Iovu H. Superporous Collagen-Sericin Scaffolds. *J Appl Polym Sci* (2013) 127:2269–79. doi:10.1002/app.37934
25. Avery D, Govindaraju P, Jacob M, Todd L, Monslow J, Puré E. Extracellular Matrix Directs Phenotypic Heterogeneity of Activated Fibroblasts. *Matrix Biol* (2018) 67:90–106. doi:10.1016/j.matbio.2017.12.003
26. Baneyx G, Baugh L, Vogel V. Fibronectin Extension and Unfolding within Cell Matrix Fibrils Controlled by Cytoskeletal Tension. *Proc Natl Acad Sci* (2002) 99:5139–43. doi:10.1073/pnas.072650799
27. Smith ML, Gourdon D, Little WC, Kubow KE, Eguiluz RA, Luna-Morris S, et al. Force-Induced Unfolding of Fibronectin in the Extracellular Matrix of Living Cells. *Plos Biol* (2007) 5:e268–2254. doi:10.1371/journal.pbio.0050268
28. Wan AM-D, Inal S, Williams T, Wang K, Leleux P, Estevez L, et al. 3D Conducting Polymer Platforms for Electrical Control of Protein Conformation and Cellular Functions. *J Mater Chem B* (2015) 3:5040–8. doi:10.1039/C5TB00390C
29. Zhang H, Hussain I, Brust M, Butler MF, Rannard SP, Cooper AI. Aligned Two- and Three-Dimensional Structures by Directional Freezing of Polymers and Nanoparticles. *Nat Mater* (2005) 4:787–93. doi:10.1038/nmat1487
30. Ren L, Tsuru K, Hayakawa S, Osaka A. Novel Approach to Fabricate Porous Gelatin-Siloxane Hybrids for Bone Tissue Engineering. *Biomaterials* (2002) 23:4765–73. doi:10.1016/S0142-9612(02)00226-0
31. Akhtar R, Sherratt MJ, Cruickshank JK, Derby B. Characterizing the Elastic Properties of Tissues. *Mater Today* (2011) 14:96–105. doi:10.1016/s1369-7021(11)70059-1
32. Wang K, Andresen Eguiluz RC, Wu F, Seo BR, Fischbach C, Gourdon D. Stiffening and Unfolding of Early Deposited-Fibronectin Increase Proangiogenic Factor Secretion by Breast Cancer-Associated Stromal Cells. *Biomaterials* (2015) 54:63–71. doi:10.1016/j.biomaterials.2015.03.019
33. Singh P, Carraher C, Schwarzbauer JE. Assembly of Fibronectin Extracellular Matrix. *Annu Rev Cel Dev. Biol.* (2010) 26:397–419. doi:10.1146/annurev-cellbio-100109-104020
34. Bachman H, Nicosia J, Dysart M, Barker TH. Utilizing Fibronectin Integrin-Binding Specificity to Control Cellular Responses. *Adv Wound Care* (2015) 4:501–11. doi:10.1089/wound.2014.0621
35. García AJ, Schwarzbauer JE, Boettiger D. Distinct Activation States of α5β1 Integrin Show Differential Binding to RGD and Synergy Domains of Fibronectin. *Biochemistry* (2002) 41:9063–9. doi:10.1021/bi025752f
36. Danen EHJ, Aota S-i., van Kraats AA, Yamada KM, Ruiter DJ, van Muijen GNP. Requirement for the Synergy Site for Cell Adhesion to Fibronectin Depends on the Activation State of Integrin α5β1. *J Biol Chem* (1995) 270:21612–8. doi:10.1074/jbc.270.37.21612
37. Sechler JL, Corbett SA, Schwarzbauer JE. Modulatory Roles for Integrin Activation and the Synergy Site of Fibronectin during Matrix Assembly. *MBoC* (1997) 8:2563–73. doi:10.1091/mbc.8.12.2563
38. Kubow KE, Klotzsch E, Smith ML, Gourdon D, Little WC, Vogel V. Crosslinking of Cell-Derived 3D Scaffolds Up-Regulates the Stretching and Unfolding of New Extracellular Matrix Assembled by Reseeded Cells. *Integr Biol* (2009) 1:635–48. doi:10.1039/b914996a


**Conflict of Interest:** The authors declare that the research was conducted in the absence of any commercial or financial relationships that could be construed as a potential conflict of interest.

The reviewer KW declared a past co-authorship with one of the authors DG to the handling editor.